NOTES AND CORRESPONDENCE

Measurement of Air–Sea Fluxes over the Indian Ocean and the Bay of Bengal

G. S. BHAT

Centre for Atmospheric and Oceanic Sciences, Indian Institute of Science, Bangalore, India

31 October 2001 and 20 May 2002

ABSTRACT

Atmospheric and oceanic data were collected in 1998 and 1999 over the tropical Indian Ocean during three cruises of the Indian research vessel *Sagar Kanya*, covering different geographic locations and seasons, including boreal winter, peak monsoon, and postmonsoon periods. The present study is mainly based on the measurements made during the three cruises. It is found that there are important differences in the near-surface characteristics during monsoon and other seasons. The largest variations in the net surface heat flux occurred during the monsoon period. The specific humidity difference between sea surface and air at 10-m height shows a strong seasonal dependence, with the lowest values observed during the monsoon period. An important finding from the ship observations is that, at a given SST, the surface air over the Indian Ocean is much warmer compared to that over other tropical oceans and the west Pacific warm pool in particular. These findings are supported by data obtained by a moored buoy in the north Indian Ocean and also from the Comprehensive Ocean–Atmosphere Data Set for the Indian Ocean.

1. Introduction

The tropical Indian Ocean is an important but poorly monitored part of the earth's climate system. In the absence of direct measurements over this ocean, surface characteristics observed over the equatorial west Pacific (e.g., Waliser and Graham 1993) have been used in some studies for calculating the surface fluxes over the Indian Ocean (e.g., Shinoda et al. 1998); however, their validity remains to be tested. In the past 3–4 yr, field experiments have been conducted on board research ships covering different parts of the tropical Indian Ocean. These include the Indian Ocean Experiment (INDOEX; e.g., Mitra 1999), the Joint Air–Sea Monsoon Interaction Experiment (JASMINE; Webster et al. 2002), and the Bay of Bengal Monsoon Experiment (BOBMEX; Bhat et al. 2001). These experiments have provided the in situ data to study the properties of the atmosphere and the ocean over the Indian Ocean. The present study is based on the measurements made during INDOEX, BOBMEX, and the Pilot Experiment for BOBMEX (hereafter referred to as PILOT; Bhat et al. 2000). These experiments were conducted during different seasons and covered different geographic locations. The main objectives of this paper are (i) to compare latent heat flux and daily net surface heat flux variations during the INDOEX, BOBMEX, and PILOT experiments; (ii) to compare tropical Indian Ocean and west Pacific characteristics, and (iii) to compare ship and the National Centers for Environmental Prediction–National Center for Atmospheric Research (NCEP–NCAR) reanalysis net daily fluxes.

Corresponding author address: Dr. G. S. Bhat, Centre for Atmospheric and Oceanic Sciences, Indian Institute of Science, Bangalore 560 012, India.
E-mail: bhat@caos.iisc.ernet.in

2. Field phase and data

Ship cruise tracks and the observation periods of INDOEX, BOBMEX, and PILOT are shown in Fig. 1. All these observations were made from the Indian research vessel *Sagar Kanya*. INDOEX was carried out in different phases spanned over a period of about 4 yr (e.g., Mitra 1999), and here the data collected during the INDOEX main phase (20 January–10 March 1999), called the INDOEX Intensive Field Phase (IFP99), are shown. ORV *Sagar Kanya* was continuously moving during IFP99, covered the latitudes 15°N–20°S in the Arabian Sea and the south Indian Ocean. In BOBMEX, carried out during the peak monsoon months of July–August 1999, the emphasis was on stationary time series measurements, and the ship was stationary at 17.5°N, 89°E from 27 July to 24 August with a break for port call from 6 to 12 August (Bhat et al. 2001). The PILOT experiment was carried out during 23 October–11 November 1998 (Bhat et al. 2000). The PILOT cruise included two 2-day time series observations at 7° and

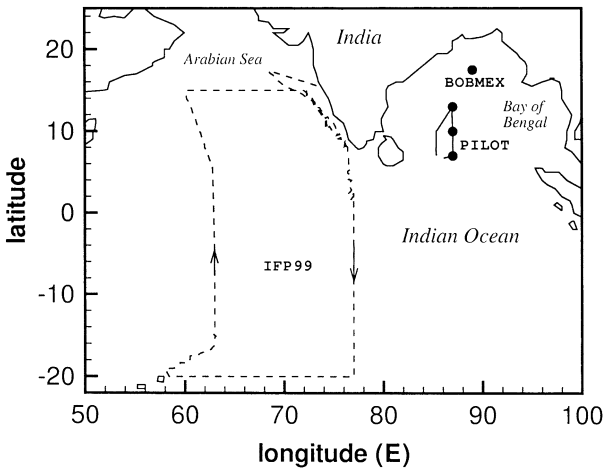

FIG. 1. Observation positions during IFP99, BOBMEX, and the PILOT cruises. Results shown refer to the data collected along the ship track and at time series stations (indicated by the filled circles). Time periods: IFP99—20 Jan–10 Mar 1999; BOBMEX—16 Jul–30 Aug 1999; PILOT—23 Oct–11 Nov 1998.

10°N and a third time series observation for a day at 13°N. These time series stations were located along 87°E latitude. For the remaining period, the ship was continuously moving (Bhat et al. 2000). In the following, IFP99 results refer to that along the cruise track of ORV *Sagar Kanya*, BOBMEX results to time series data in the north Bay of Bengal at 17.5°N, 89°E, and PILOT results include the data at the time series stations and along the cruise track shown in Fig. 1.

The same set of sensors and instruments were used for measuring air temperature, relative humidity, wind speed, and radiation in all three cruises. Similar pre- and postcruise sensor calibration procedures were adopted. The sensor installations on the ship, data acquisition, and processing procedures were also identical. These ensured uniformity in the measurements among the three cruises. The details pertaining to the sensors used, experimental arrangement on the ship, sensor calibration, and intercomparison during BOBMEX are given in Bhat et al. (2001). In brief, a sonic anemometer (manufactured by Metek), Gill anemometer (R. M. Young, Co.), and humicap relative humidity and PRT temperature sensors (R. M. Young Co., contained in a Young radiation shield) were mounted at a mean height of 11.5 m above the sea surface on a boom that stretched 8 m ahead of the ship. Incoming components of shortwave and longwave radiation were measured using Eppley radiation instruments. Rainfall was measured using an automatic rain gauge (R. M. Young Co.). During BOBMEX, the outgoing component of longwave radiation and reflected shortwave radiation were also measured.

3. Results

The synoptic conditions during the IFP99, BOBMEX, and PILOT experiments were distinct. During the IFP99 period (January–March), convection is normally active between 5°N and 12°S. However, along the cruise track, no major convective systems were present, and the weather conditions were representative of weak/suppressed convective conditions. BOBMEX was planned during peak monsoon months (July–August), a period characterized by the frequent formation of monsoon systems, extensive cloud cover, and intense precipitation. During BOBMEX, both active and weak phases of convection were encountered (Bhat et al. 2001). October–November is a favorable time for the formation of tropical cyclones over the Bay of Bengal, and convection was active in and around the study area during the PILOT experiment (Kalsi 2000). Thus, the three experiments covered three different climatic conditions over the north Indian Ocean. Figure 2a shows the variation of sea surface temperature (SST), wind speed, hourly precipitation, and latent heat flux (LHF) along the ship track during IFP99. SST was above the convection threshold value of 27.5°C (Gadgil et al. 1984; Graham and Barnett 1987) between 10°N and 12°S. Wind speeds varied from less than 2 to more than 12 m s^{-1}. Only few convective and rainfall events were observed, and the maximum rainfall measured was less than 30 mm day^{-1} during the entire cruise. LHF is computed here using the Zeng et al. (1998) bulk method. During the BOBMEX and PILOT cruises, an IR hygrometer (fast humidity instrument) was used, and the computation of LHF using eddy-correlation and inertial-dissipation methods (i.e., direct methods) is in progress. Results obtained so far show good agreement between the fluxes from bulk and direct methods in the mean. The results shown here are based on the bulk method. LHF varied between 30 and 320 W m^{-2} during IFP99, with average values close to 125 W m^{-2} during both the forward (days 21–40, hereafter days mean Julian days) and return (days 50–69) cruises.

Figure 2b shows SST, wind speed, hourly precipitation, and LHF during BOBMEX. Three monsoon systems formed between days 205 and 220, and the period between days 230 and 236 was a weak phase of convection in the region (Bhat et al. 2001). SST was above the convection threshold except for a brief period on Julian day 228 (16 August). The decrease in SST coincided with intense convective events, and warming took place during weak periods of convection. The average wind speeds were much stronger during BOBMEX compared to that during IFP99. More than 50 mm of rainfall was recorded on four days. The average LHF was larger during the first half (days 208–218) compared to that during most of the second half (days 226–236). Figure 2c shows the surface conditions during PILOT. The average SST was more than 29°C and the winds were weaker. Frequent showers were observed, but the total daily rainfall was small (only on one day did it exceed 20 mm). LHF varied between 45 and 290 W m^{-2}, with an average around 140 W m^{-2}.

The daily net surface heat flux Q_{net}, defined as

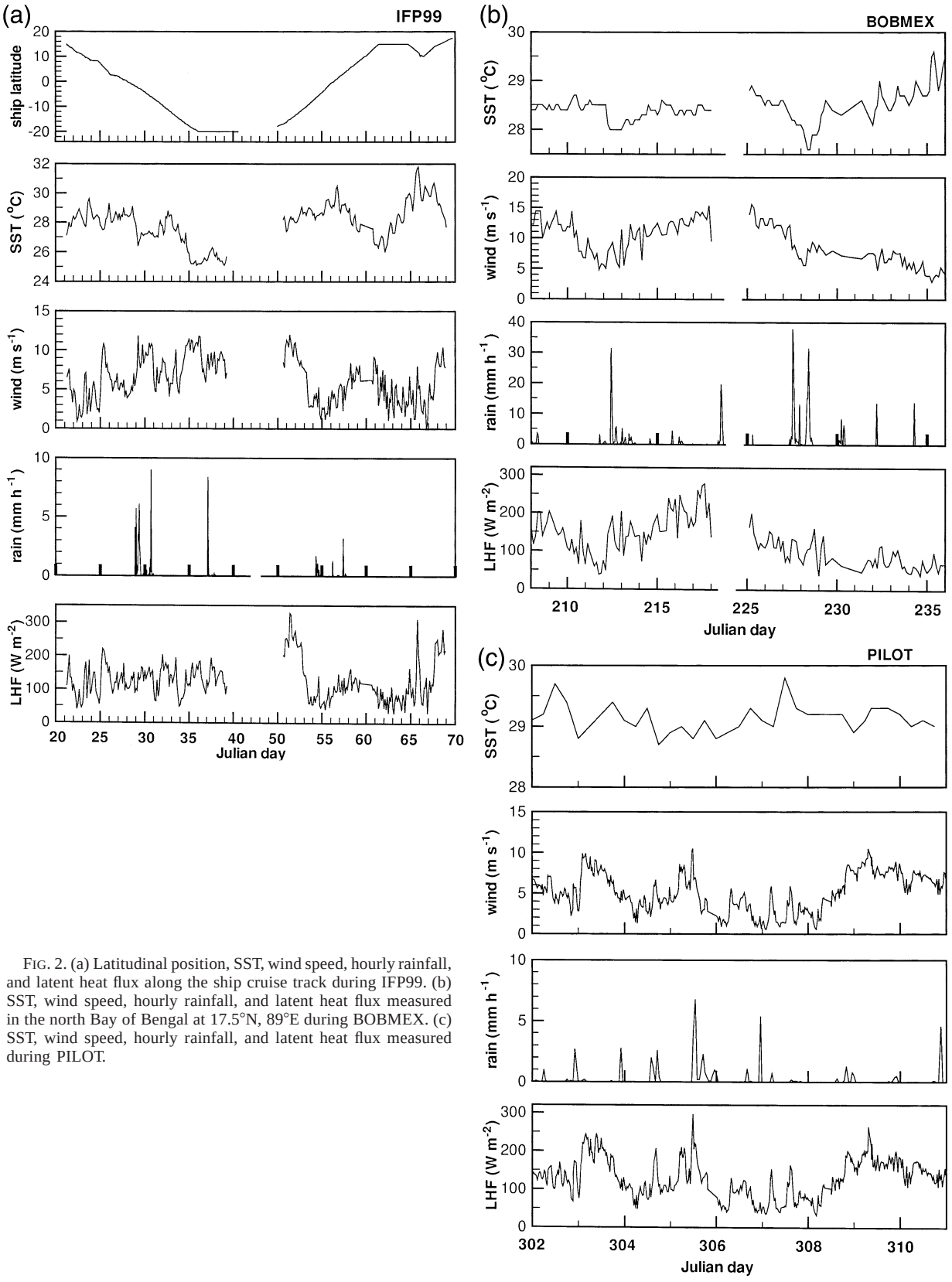

FIG. 2. (a) Latitudinal position, SST, wind speed, hourly rainfall, and latent heat flux along the ship cruise track during IFP99. (b) SST, wind speed, hourly rainfall, and latent heat flux measured in the north Bay of Bengal at 17.5°N, 89°E during BOBMEX. (c) SST, wind speed, hourly rainfall, and latent heat flux measured during PILOT.

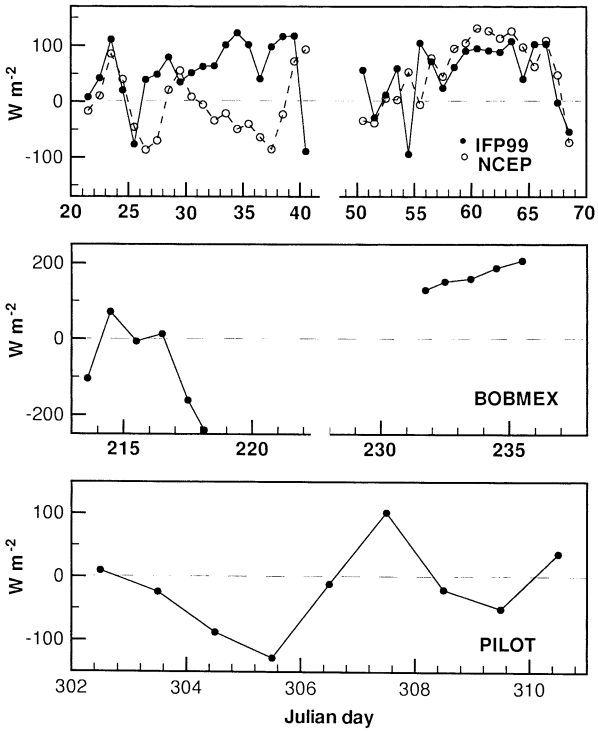

FIG. 3. Variation of daily net heat flux for (top) IFP99, (middle) BOBMEX, and (bottom) PILOT. Also shown in (top) is NCEP reanalysis net heat flux.

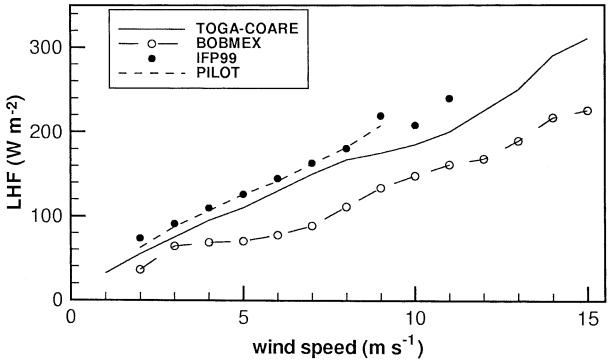

FIG. 4. Mean variation of the latent heat flux with wind speed. TOGA COARE data are taken from Fig. 11 of Fairall et al. (1996).

Q_{net} = NSW − NLW + LHF + SHF), where NSW is net shortwave radiation, NLW is net longwave radiation, and SHF is sensible heat flux, is shown in Fig. 3. (Flux into the ocean is taken as positive.) The net heat flux basically followed the synoptic conditions. When convection was active, depleted shortwave radiation and increased LHF due to stronger winds resulted in substantial net heat loss. The reverse was taking place during the weak phase of convection. During IFP99, net heat flux varied from −90 to 120 W m^{-2}. The corresponding range was −240–220 W m^{-2} and −140–100 W m^{-2}, respectively, during BOBMEX and PILOT. During JASMINE, carried out over the Bay of Bengal during April–June 1999, net heat flux values ranged from −150 to 125 W m^{-2}. Therefore, the largest variations in the net heat flux among the recent experiments over the Indian Ocean are seen during the peak monsoon period in the north Bay of Bengal. Webster et al. (2002) report that the intraseasonal variability of the fluxes observed during JASMINE was generally larger than that encountered during the Tropical Ocean Global Atmosphere Coupled Ocean–Atmosphere Response Experiment (TOGA COARE) in the western Pacific Ocean. Although the present time series are not long enough to clearly bring out the intraseasonal variations, the range of BOBMEX net heat flux variations are larger than those observed during JASMINE, and support the observation made by Webster et al. (2002) that variations in the net heat flux are large over the Bay of Bengal during the monsoon.

The NCEP reanalysis daily net surface heat flux, corresponding to the grid box where the ship was located on the respective day of observation during IFP99, is shown in Fig. 3 (top). In general, the agreement between the two is better in the north Indian Ocean and poorer in the south Indian Ocean. When the individual components of the heat flux are examined, it is observed that ship and NCEP reanalysis net longwave, latent heat, and sensible heat fluxes are in reasonable agreement with each other (Bhat et al. 2003). Good and poor agreement in Q_{net} mainly resulted from differences in the net shortwave radiation, the largest component of Q_{net} (Bhat et al. 2003).

It is observed from Figs. 2a–c that despite stronger winds, the LHF was not correspondingly higher during BOBMEX. This aspect is more clearly seen in the variation of LHF with wind speed shown in Fig. 4, where the mean values of LHF in each 1 m s^{-1} wind speed interval are plotted. Also shown in Fig. 4 are TOGA COARE data interpolated from Fig. 11 of Fairall et al. (1996). [The coefficients in the Zeng et al. (1998) bulk algorithm (which is used in the present work) have been tuned so as to agree with the TOGA COARE fluxes.] In the IFP99 results shown hereafter, observations within 12°N–12°S only are included. The latent heat fluxes at a given wind speed are comparable during TOGA COARE, IPF99, and PILOT; however, those during BOBMEX are lower by 30%–40%. The factor responsible for the lower values of LHF during BOBMEX is the high amount of water vapor in the air during the monsoon period. While typical values of relative humidity over the tropical oceans are 75%–80%, those observed during BOBMEX were often in the 85%–90% range. As a result, the specific humidity difference between the sea surface (saturated at SST) and air at 10-m height was typically in the 3–4 g kg^{-1} range during BOBMEX compared to values of 5–7 g kg^{-1} normally observed over the tropical oceans. Therefore, although the winds were much stronger during the summer mon-

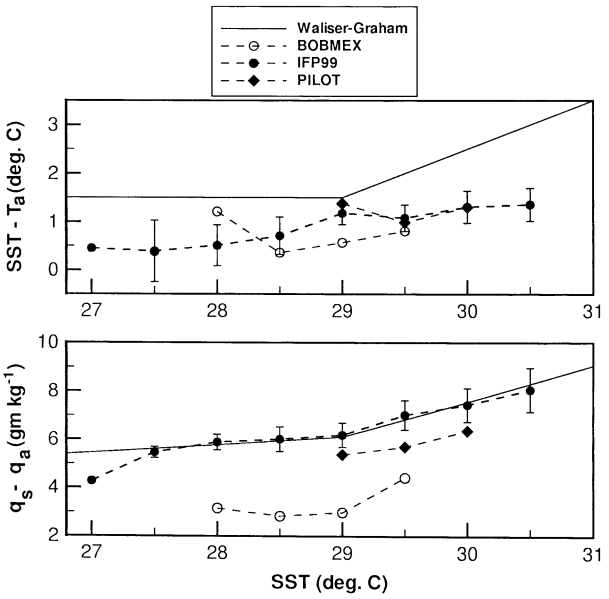

FIG. 5. Variation of air–sea (top) temperature and (bottom) specific humidity differences with SST. The continuous line is Eq. (1) based on Waliser and Graham's (1993) work. For the IFP99 data alone, error bars corresponding to one std dev are shown.

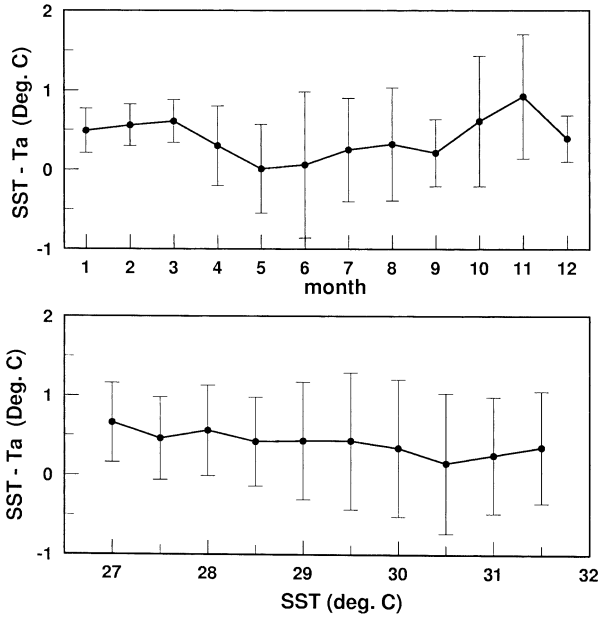

FIG. 6. Monthly variation of air–sea temperature difference based on the buoy data at 13°N, 89°E. Error bars denote one std dev.

soon, the surface cooling due to evaporation of water was not proportionately higher.

Atmospheric models often need air–sea temperature difference ΔT (=SST $-$ T_a, where T_a is the air temperature at 10 m height), and specific humidity difference Δq (=$q_s - q_a$, where q_s and q_a are, respectively, saturation specific humidity at the ocean surface and specific humidity of air at 10-m height) as functions of other observables. For example, based on the data over the tropical west Pacific, Waliser and Graham (1993) suggested the following empirical relations for ΔT and Δq variations with SST:

$$\Delta T = \begin{cases} 1.5 & \text{for SST} < 29^\circ\text{C} \\ \text{SST} - 27.5 & \text{for SST} \geq 29^\circ\text{C} \end{cases}$$

$$\Delta q = 0.98 q_s(\text{SST}) - 0.8 q_s(T_a). \quad (1)$$

The factor 0.98 accounts for the effect of salinity on the saturation vapor pressure of water over the ocean, and 0.8 implies 80% relative humidity for air at 10-m height. The variations of mean ΔT and Δq with SST (calculated for each 0.5°C SST interval) for the Indian Ocean are shown in Fig. 5. Values of ΔT over the Indian Ocean are much smaller compared to that over the west Pacific at a given SST—while the air–sea temperature difference observed over the tropical oceans is typically 1°–2°C (Slutz et al. 1985; Weller and Anderson 1996), that over the Indian Ocean is typically in the 0.4°–0.7°C range. A strong seasonal dependence is seen in the variation of Δq with SST over the Indian Ocean. While the average Δq very closely followed the SST dependence given by (1) during IFP99 at SSTs above 28°C, BOBMEX values were lower by 30%–50%, and those during PILOT were marginally lower but not very different from IFP99 values.

The results shown in Fig. 5 are based on limited observations over the tropical Indian Ocean at different locations. Are the features seen in Fig. 5 representative of the characteristics of the Indian Ocean in general or merely specific to the particular observation periods? To address this issue, it is necessary to consider data spanning a longer time period and/or a larger area. It is desirable that the data are based on direct observations, but as pointed out in the introduction, accurate and detailed observations have been lacking for the Indian Ocean. Here, I consider two data sources, namely, moored buoy data in the Bay of Bengal and the Comprehensive Ocean–Atmosphere Data Set (COADS). Moored buoys have been deployed and maintained in the north Indian Ocean since 1997 by the National Institute of Ocean Technology, Chennai, India (Premkumar et al. 2000). Air temperature (measured at 3.2-m height above the surface) and SST (measured at a depth of 2.2 m below the surface) are reported every 3 h. Owing to pilferage there are gaps in the buoy data, and here the data from the buoy located at 13°N, 87°E are selected, as continuous observations covering all 12 months (September 1997–September 1998) are available. Intercomparison experiments carried out during BOBMEX showed buoy temperatures in good agreement with ship data (Bhat et al. 2001). Thus, buoy data are reliable, however, humidity is not measured from these buoys at present; hence, only ΔT variation can be studied. Figure 6 shows the variation of monthly mean ΔT derived from the buoy data. The seasonal variation

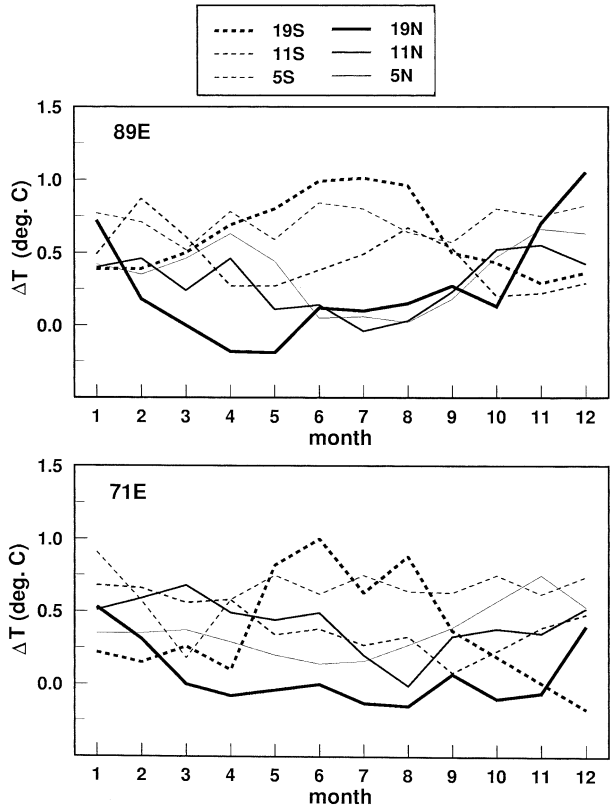

FIG. 7. Monthly variation of mean air–sea temperature difference derived from the COADS dataset for the period 1900–92.

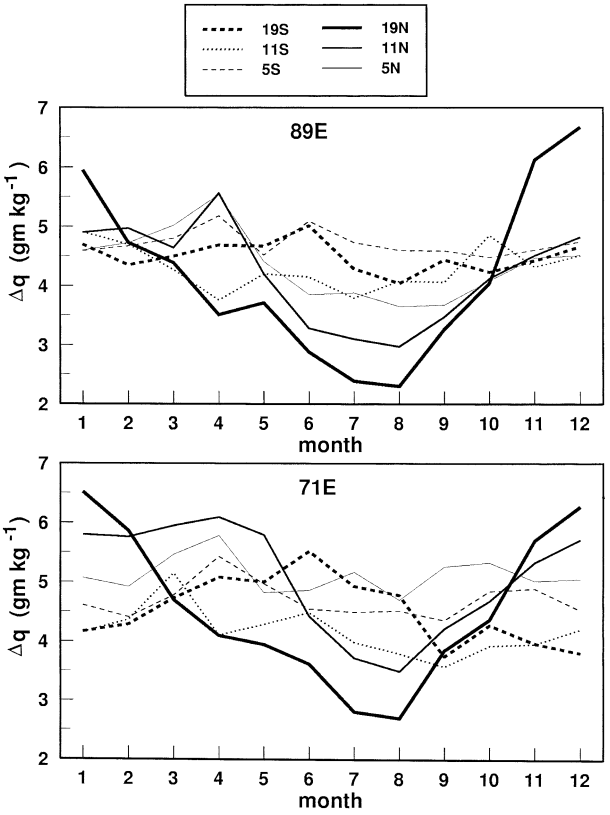

FIG. 8. Monthly variation of mean air–sea specific humidity difference Δq derived from the COADS dataset for the period 1900–92.

in ΔT is evident in Fig. 6 where values less than 0.5°C occurred during the May–September period and larger values occurred from October to December. The mean value of 0.4°C during July–August (in 1998) is comparable to that observed during BOBMEX in the north Bay of Bengal in 1999. Also it is observed from Fig. 6 (bottom) that mean ΔT is around 0.5°C and shows little variation with SST.

Here, COADS data are downloaded online at http://iridl.ldeo.columbia.edu/SOURCES/. COADS data are not as accurate as those from research ships and moored buoys; however, when long-term averages are taken, errors tend to reduce, and the means bring out the broad characteristics of the region. Monthly variations of the mean values of ΔT and Δq using the monthly mean fields from COADS data for the period January 1900–December 1992 along two longitudes (71°–89°E) are shown in Figs. 7 and 8. At both longitudes, the largest value of ΔT is less than 1°C with lower values occuring in the summer hemisphere. In the north Indian Ocean, seasonal variations of ΔT and Δq become more prominent with increasing distance from the equator. Figures 7 and 8 are representative of the variations in ΔT and Δq observed over the Indian Ocean. For example, Figs. 9a and 9b show spatial distributions of ΔT and Δq for the months of January and August. The contrasts in ΔT and Δq fields between January and August over the north Indian Ocean are clearly brought out in Fig. 9. The changes over the south Indian Ocean are relatively small. It is also clear from Fig. 9 that values of both ΔT (less than 1°C) and Δq (3–6 g kg^{-1}) are low compared to the corresponding values over the west Pacific.

4. Discussion

Results presented in the previous section clearly show that the near-surface characteristics over the tropical Indian Ocean are distinct, and in particular, values of ΔT and Δq are often much smaller when compared to those over the west Pacific warm pool. The underlying mechanism that produces these differences is not clear. Some insight is gained by considering the energy and water vapor balance of the atmospheric mixed layer. Here only the water vapor budget is examined and the energy balance has been given in Bhat (2003). For the mixed layer, conservation of water vapor per unit area (under suppressed and shallow convective conditions) can be expressed as (Fig. 10)

$$d(\rho_1 H q_1)/dt = Q_{\text{fs}} + Q_{\text{ad}} - (\rho_t w_t \Delta q_t + \rho_t w_c' q'), \quad (2)$$

where H is the mixed layer height, ρ is density of air, Q_{fs} is the flux of water vapor at the surface, Q_{ad} is the horizontal advection, w_t is the large-scale subsidence

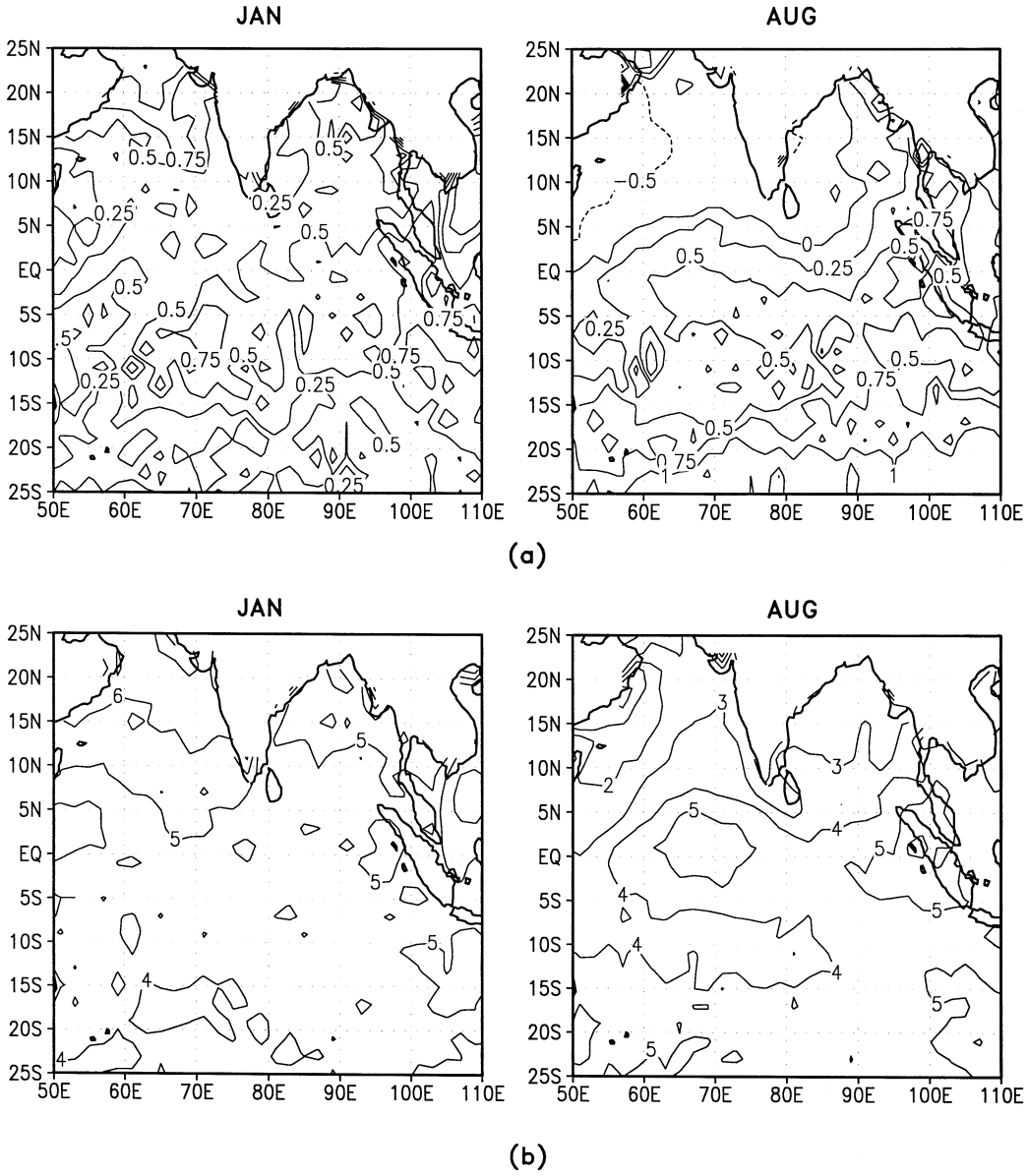

FIG. 9. The spatial variation of (a) ΔT and (b) Δq during Jan and Aug obtained from COADS data.

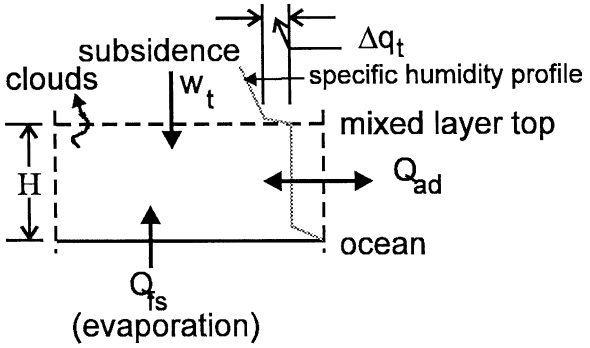

FIG. 10. A schematic of the control volume for calculating the moisture budget of the atmospheric mixed layer during suppressed convective conditions.

velocity at the top of the mixed layer, Δq_t is the decrease in specific humidity across the mixed layer top (Fig. 10), and $w_c'q'$ represents the vertical transport due to cumulus cloud activity. The subscripts 1 and t, respectively, refer to properties of the mixed layer air and that at its top. Subsidence tends to decrease the humidity of the mixed layer (Betts and Ridgway 1988). Similarly, cumulus cloud activity decreases the mean specific humidity of the mixed layer by transporting moist air upward and bringing down drier air from above. Mainly evaporation from the surface tends to increase the humidity of the mixed layer. According to the bulk aerodynamic formulas (e.g., Zeng et al. 1998), the moisture flux from the surface is given by

$$Q_{fs} = \rho_s C_d U \Delta q, \quad (3)$$

where ρ_s is density of the air at the surface, C_d is the drag coefficient, and U is the mean wind speed.

Over the tropical oceans, the time variations in q_1 and H under suppressed convective conditions are small. Therefore, in the absence of horizontal advection and cumulus transport of moisture, we can expect a quasi equilibrium in which subsidence drying is balanced by evaporation at the surface. Subsidence drying is related to the rate of subsidence and the vertical profile of humidity, which are controlled by the large-scale dynamical and thermodynamical processes. The surface moisture flux is governed by local wind speed U, Δq, and the stability of the surface layer (by influencing C_d). If the large-scale conditions do not change rapidly, then we can expect the surface evaporation to adjust to maintain the water vapor equilibrium of the mixed layer, and

$$\Delta q = (\rho_t w_t \Delta q_t + \rho_t w_c' q')/(\rho_s C_d U). \quad (4)$$

Note that in the absence of convective clouds the $\rho_t w_c' q'$ term is zero. From (4) we see that Δq is directly proportional to the rate of subsidence at the top of the mixed layer and inversely proportional to the wind speed. We can expect Δq_t to depend on the synoptic conditions with larger values being associated with clear-sky conditions and when the mixed layer is capped by an inversion. Here C_d (1.2–1.3 $\times$ 10^{-3}; e.g., Fairall et al. 1996) is strictly not a constant but its variations may be ignored for the present purpose for wind speeds above 2 m s^{-1}.

With the ship data, variation of Δq with wind speed can be studied as shown by Fig. 11. During IFP99, Δq seems to decrease inversely with the wind speed. A slightly decreasing trend in Δq with wind speed is observed during PILOT. The Δq also decreased with wind speed during BOBMEX, however, only at wind speeds below 8 m s^{-1}. During BOBMEX, the low wind speed regime (called regime 1 in Fig. 11) generally corresponded to the weak phase of convection and the high wind speed regime 2 to the active phase of convection. When convection is active, convective clouds remove the moisture from the mixed layer and transport it to higher levels and the $w_c' q'$ term can become significant and overcome the inverse U influence. Another important process not included in (4) is the role of precipitating clouds, which can dry the mixed layer when downdrafts are strong (Betts 1976). Therefore, (4) cannot be used when precipitating clouds are present. On the other hand, for clear-sky and suppressed convective conditions, (4) describes the factors influencing Δq. Analysis of the relative magnitudes of the terms on the right-hand side of (4) is beyond the scope of the present study, but when carried out, will provide more insight into the differences between the Indian Ocean and west Pacific, and also the seasonal variation over the Indian Ocean itself. For example, vertical temperature and humidity profiles during BOBMEX rarely showed a capping inversion and, therefore, values of Δq_t were small (Bhat and Chandrasekhar 2001). This could have been one of reasons for low values of Δq observed during BOBMEX.

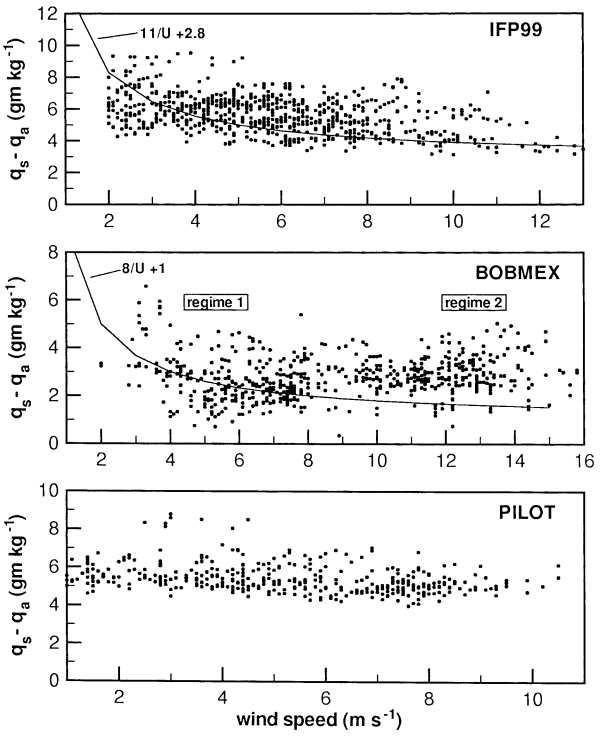

FIG. 11. Variation of Δq with wind speed during (top) IFP99, (middle) BOBMEX, and (bottom) PILOT experiments.

5. Summary

The emphasis in the recent literature regarding air–sea fluxes over the tropical oceans has been on obtaining accurate values of the drag coefficients for use in bulk aerodynamic formulas under different wind speed and stability conditions. The present study shows that it is equally important to consider the spatiotemporal variations in ΔT and Δq fields over the Indian Ocean. Important conclusions are as follows:

1) The variation in the net daily heat flux over the tropical Indian Ocean is largest during the Indian summer monsoon period.
2) The surface air over the Indian Ocean is warmer compared to other tropical oceans at a given SST.
3) The air–sea specific humidity difference Δq is significantly low when compared to that over the west Pacific warm pool region during the Indian summer monsoon. In the north Indian Ocean Δq shows stronger seasonal dependence with increasing distance from the equator.

Acknowledgments. This work was partially supported by a grant from the Department of Science and Tech-

nology, New Delhi, India, and I would like to thank the agency for their support. I would also like to thank the various Indian government agencies that supported INDOEX and BOBMEX. Prof. Sulochana Gadgil is acknowledged for her encouragement and valuable advice while this work was being carried out. My thanks are also due to all those who were involved in the INDOEX and BOBMEX programmes and helped to collect data. The National Institute of Ocean Technology, Chennai, India, provided the buoy data in the Bay of Bengal. I would also like to thank the two anonymous referees whose critical reviews led to improvements in this manuscript.

REFERENCES

Betts, A. K., 1976: The thermodynamic transformation of the tropical subcloud layer by precipitation and downdrafts. *J. Atmos. Sci.*, **33,** 1008–1020.

——, and W. Ridgway, 1988: Coupling of the radiative, convective and surface fluxes over the equatorial Pacific. *J. Atmos. Sci.*, **45,** 522–536.

Bhat, G. S., 2003: Near surface variations and surface fluxes over the North Bay of Bengal during the 1999 Indian Summer Monsoon. *J. Geophys. Res.*, **107,** 4336, doi:10.1029/2001JD000382.

——, and C. P. Chandrasekhar, 2001: The Bay of Bengal Monsoon Experiment: BOBMEX. *ORV Sagar Kanya* radiosonde profiles. Rep. No. ICRP/IISC/CAOS/02, Centre for Atmospheric Oceanic Sciences, Indian Institute of Science, Bangalore, India, 200 pp.

——, S. Ameenulla, M. Venkataramana, and K. Sengupta, 2000: Atmospheric boundary layer characteristics during the BOBMEX-Pilot experiment. *Proc. Indian Acad. Sci. (Earth Planet. Sci.),* **109,** 229–237.

——, and Coauthors, 2001: BOBMEX—The Bay of Bengal Monsoon Experiment. *Bull. Amer. Meteor. Soc.,* **82,** 2217–2243.

——, M. A. Thomas, J. V. S. Raju, and C. P. Chandrasekhara, 2003: Surface characteristics over the central Indian Ocean observed during INDOEX IFP99. *Bound.-Layer Meteor.,* in press.

Fairall, C. W., E. F. Bradley, D. P. Rogers, J. B. Edson, and G. S. Young, 1996: Bulk parameterization of air–sea fluxes for Tropical Ocean Global Atmosphere Coupled Ocean–Atmosphere Response Experiment. *J. Geophys. Res.,* **101,** 155–192.

Gadgil, S., P. V. Joseph, and N. V. Joshi, 1984: Ocean–atmosphere coupling over monsoon regions. *Nature,* **312,** 141–143.

Graham, N. E., and T. P. Barnett, 1987: Sea surface temperature, surface wind divergence and convection over tropical oceans. *Science,* **238,** 657–659.

Kalsi, S. R., 2000: Synoptic weather conditions during the pilot study of Bay of Bengal Monsoon Experiment (BOBMEX) *Proc. Indian Acad. Sci. (Earth Planet. Sci.),* **109,** 211–220.

Mitra, A. P., 1999: INDOEX (India) introductory note. *Curr. Sci.,* **76,** 886–889.

Premkumar, K., M. Ravichandran, S. R. Kalsi, D. Sengupta, and S. Gadgil, 2000: First results from a new observational system over the Indian seas. *Curr. Sci.,* **78,** 323–331.

Shinoda, T., H. H. Hendon, and J. Glick, 1998: Intraseasonal variability of surface fluxes and sea surface temperature in the tropical western Pacific and Indian Oceans. *J. Climate,* **11,** 1685–1702.

Slutz, R. J., S. J. Lubker, J. D. Hiscox, S. D. Woodruff, R. L. Jenne, D. H. Joseph, P. M. Steurer, and J. D. Elms, 1985: COADS: Comprehensive Ocean Atmosphere Data Set. Release 1, NOAA Environmental Research Laboratories, Boulder, CO, 262 pp.

Waliser, D. E., and N. E. Graham, 1993: Convective cloud system and warm-pool sea surface temperatures; Coupled interactions and self-regulation. *J. Geophys. Res.,* **98,** 12 881–12 893.

Webster, P. J., and Coauthors, 2002: The JASMINE Pilot Study. *Bull. Amer. Meteor. Soc.,* **83,** 1603–1630.

Weller, R. A., and S. P. Anderson, 1996: Surface meteorology and air–sea fluxes in the western equatorial Pacific warm pool during the Coupled Ocean–Atmosphere Response Experiment. *J. Climate,* **9,** 1959–1990.

Zeng, X., M. Zhao, and R. E. Dickinson, 1998: Intercomparison of bulk aerodynamic algorithms for computation of sea surface fluxes using TOGA COARE and TAO data. *J. Climate,* **11,** 2628–2644.